JOURNAL OF MATERIALS SCIENCE 28 (1993) 917–926

The microhardness indentation load/size effect in rutile and cassiterite single crystals

H. LI*, R. C. BRADT
The Mackay School of Mines, University of Nevada, Reno, NV 89557, USA

The microhardness indentation load/size effect (ISE) on the Knoop microhardness of single crystals of TiO_2 and SnO_2 has been investigated. Experimental results have been analysed using the classical power law approach and from an effective indentation test load viewpoint. The Hays/Kendall concept of a critical applied test load for the initiation of plastic deformation was considered, but rejected to explain the ISE. A proportional specimen resistance (PSR) model has been proposed that consists of the elastic resistance of the test specimen and frictional effects at the indentor facet/specimen interface during microindentation. The microhardness test load, P, and the resulting indentation size, d, have been found to follow the relationship

$$P = a_1 d + a_2 d^2 = a_1 d + (P_c/d_0^2) d^2$$

The ISE is a consequence of the indentation-size proportional resistance of the test specimen as described by a_1. a_2 is found to be related to the load-independent indentation hardness. It consists of the critical indentation load, P_c, and the characteristic indentation size, d_o.

1. Introduction

Of all of the testing techniques which have been applied to assess the mechanical properties of materials, indentation hardness testing is probably the one in most widespread use [1–5]. Applications of microhardness indentation techniques, however, experience the indentation load/size effect at low levels of the testing load. This is known as the ISE and has been traditionally described through the application of the power law

$$P = Ad^n \quad (1)$$

where P is the indentation test load and d is the resulting indentation size. A and n are descriptive parameters derived from the curve fitting of experimental results. Equation 1 is sometimes referred to as Meyer's law [6]. For virtually all materials, the power law exponent, n, is experimentally observed to be between 1 and 2, which indicates that lower indentation test loads result in higher apparent microhardnesses. This load dependence of hardness has been frequently reported [7–15].

The indentation load/size effect (ISE) on the microhardness has been considered on the basis of a variety of phenomena, including work hardening during indentation [2, 3], the load to initiate plastic deformation [5], indentation elastic recovery [12], the activation energy for dislocation nucleation [13], surface dislocation pinning [14, 15] and plastic deformation band spacing [16]. However, neither an explanation of the physical meaning of the power law exponent, the n value, nor the cause of the indentation load/size effect has been satisfactorily achieved. This paper addresses those issues, examining extensive Knoop indentation measurements for two rutile-structure single crystals, TiO_2 and SnO_2 [10, 11].

2. Experimental results of the ISE

The phenomenon of the ISE exists for a variety of indentor geometries, including the Brinell, Vickers and Knoop. Application of Equation 1 to the results yields an n value that is less than 2, indicative of an increasing apparent microhardness at lower indentation test loads. To examine the ISE critically, it is necessary to evaluate an extensive set of experimental microhardness measurements on one material or related materials with the same crystal structure. It is also desirable to avoid the complications which are introduced by the grain boundaries in polycrystalline structures and the phase boundaries in multiphase or composite structures. An obvious choice is one of single-crystal results. Because of the availability of extensive data for rutile (TiO_2) [10] and cassiterite (SnO_2) [11], they have been chosen for the analyses applied in this paper. Previous studies of these single-crystals have addressed the microhardness anisotropies on different crystallographic planes and for different crystallographic directions. Those features will not be reviewed; only the load dependencies of the microhardnesses will be considered.

Fig. 1 illustrates the relationship found between the coefficient, A, and the power law exponent, n, when the ISE phenomenon for TiO_2 and SnO_2 is addressed

Present address: Materials Research Center, Rensselaer Polytechnic Institute Troy, New York 12180-3590, USA

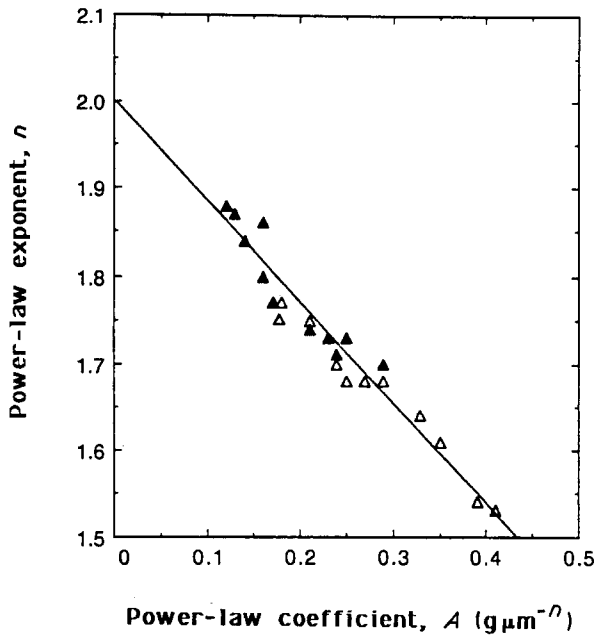

Figure 1 Relationship between the power-law parameters A and n for single crystals of (△) TiO_2 and (▲) SnO_2.

in terms of Equation 1. The individual A and n values are summarized in Table 1. Regression analysis yields an intercept of $n = 2.00 \pm 0.04$ for $A = 0$. Because an n-value of 2 is expected in the absence of an ISE, these single crystal results are consistent with the power-law description of the load dependence of the microhardness of these crystals. Sargent and Page [7] have considered several "n value versus ln A" relationships in an attempt to ascertain any possible microstructural effects on these power-law parameters. In their summary study of polycrystalline materials, a trend of n versus ln A was identified. Lower n-values are related to higher A or ln A values as the grain size increases, which relates to lower microhardnesses. They interpreted this observation as a grain-size weakening process. Later Sargent [17] associated the power-law n-value with his definition of a "standard" hardness value, H_s, and noted that lower n values are often associated with higher, H_s, values. The power-law results from these rutile structure crystals are in general agreement with the concepts advanced by Sargent and Page that there exists a basic relationship between the parameters A and n. The inverse linear relationship between the two parameters shown in Fig. 1 confirms the previously reported finding by Sargent and Page [7], although the degree of correlation which is evident for the single crystals in Fig. 1 is not revealed for the polycrystalline materials. This is probably because the microstructural effects of the polycrystalline specimens are superimposed upon the ISE.

The experimental results and discussion mentioned above verify that the ISE of rutile and cassiterite single crystals are well described using Equation 1. Unfortunately, none of these results provides a basic understanding for the two power-law parameters, A and n, nor to their relationship. It is necessary to progress beyond the power-law description to achieve an understanding of the ISE.

2.1. The Hays/Kendall approach to the ISE

Hays and Kendall [5] have considered the ISE for the Knoop microhardness of a number of metals. They advanced the concept that there exists a minimum level of the indentation test load, W, below which plastic deformation does not initiate, but only elastic deformation occurs. This has been observed by Gane and Bowden [18], who reported that there is a sudden indentor penetration into the surface of gold specimens at a nominal load level. Before the indentor achieves that critical indentation load, however, the indentation size does not increase with an increase of the test load. According to Hays and Kendall, the experimentally measured indentation size is not directly related to P, the applied indentation load, but

TABLE I The power-law parameters for single crystals of TiO_2 and SnO_2

$(h\ k\ l)[u\ v\ w]$	TiO_2		SnO_2	
	A (g μm^{-n})	n	A (g μm^{-n})	n
(1 0 0)				
[0 0 1]	0.21 ± 0.03	1.75 ± 0.02	0.25 ± 0.03	1.73 ± 0.02
[0 1 1]	0.25 ± 0.03	1.68 ± 0.01	0.14 ± 0.02	1.84 ± 0.03
[0 1 0]	0.15 ± 0.03	1.73 ± 0.01	0.17 ± 0.03	1.77 ± 0.02
(1 1 0)				
[0 0 1]	0.29 ± 0.02	1.68 ± 0.02	0.16 ± 0.02	1.80 ± 0.02
[1 $\bar{1}$ 1]	0.35 ± 0.02	1.61 ± 0.01	0.21 ± 0.02	1.74 ± 0.01
[1 $\bar{1}$ 0]	0.33 ± 0.01	1.64 ± 0.01	0.24 ± 0.01	1.71 ± 0.01
(0 0 1)				
[1 0 0]	0.41 ± 0.01	1.53 ± 0.02	0.12 ± 0.01	1.88 ± 0.02
[1 1 0]	0.18 ± 0.02	1.77 ± 0.02	0.16 ± 0.01	1.86 ± 0.02
[0 1 0]	0.39 ± 0.03	1.54 ± 0.01	0.13 ± 0.01	1.87 ± 0.01
(1 1 1)				
[1 $\bar{1}$ 0]	0.24 ± 0.02	1.69 ± 0.01	0.23 ± 0.01	1.73 ± 0.02
[$\bar{1}$ $\bar{1}$ 2]	0.27 ± 0.02	1.68 ± 0.01	0.29 ± 0.02	1.70 ± 0.02

rather to the effective indentation test load, defined as $(P - W)$ where W is the material resistance to the initiation of plastic flow, as previously described.

Hays and Kendall proposed that the relationship between the indentation test load and the indentation size is not that of the original power law, but rather

$$(P - W) = Kd^2 \quad (2a)$$

which can be rearranged to

$$P = W + Kd^2 \quad (2b)$$

where K is a constant. This form of the test load/indentation size relationship suggests that Kick's law is fundamental, always yielding an exponent that is equal to 2. It implies that the power law exponent, or n-value, is not a material property, but is rather without any fundamental physical significance. The experimental microhardness data for the TiO_2 and SnO_2 single crystals allows for a critical evaluation of the Hays and Kendall concept.

Fig. 2 illustrates the application of Equation 2b as P versus d^2 to the TiO_2 and SnO_2 single-crystal results for their (1 0 0) planes. It is evident that a linear relationship exists and that the slope varies significantly for the different indentor orientations. Although the intercepts appear to be nearly the same, this latter point is actually an illusion of the scale of the figure. Regression analyses indicate that both the intercepts and the slopes vary considerably. Table II summarizes the plastic flow initiation loads, the W values, determined from the regression analyses and the slopes of P versus d^2 for the two crystals. Both values are anisotropic. The magnitude of the plastic flow initiation load, W, is surprisingly large, a level which is significant when compared with the applied indentation test loads. However, it is similar in magnitude to the material resistance loads reported by Hays and Kendall for metals.

TABLE II Parameters of the Hays/Kendall approach for single crystals of TiO_2 and SnO_2

$(h\ k\ l)[u\ v\ w]$	TiO_2		SnO_2	
	W (g)	K[a] (g μm^{-2})	W (g)	K[a] (g μm^{-2})
(1 0 0)				
[0 0 1]	16.3 ± 0.7	0.07	18.2 ± 0.6	0.08
[0 1 1]	21.0 ± 0.8	0.06	10.0 ± 0.7	0.07
[0 1 0]	17.7 ± 0.7	0.04	14.8 ± 0.4	0.06
(1 1 0)				
[0 0 1]	21.1 ± 0.6	0.07	13.0 ± 0.2	0.07
[1 $\bar{1}$ 1]	26.1 ± 0.8	0.06	16.9 ± 0.8	0.07
[1 $\bar{1}$ 0]	26.4 ± 0.7	0.07	18.8 ± 0.9	0.07
(0 0 1)				
[1 0 0]	30.9 ± 0.5	0.05	7.8 ± 0.5	0.07
[1 1 0]	14.7 ± 0.5	0.06	9.2 ± 0.4	0.09
[0 1 0]	29.5 ± 0.6	0.05	7.9 ± 0.8	0.07
(1 1 1)				
[1 $\bar{1}$ 0]	18.1 + 0.4	0.06	17.5 ± 0.5	0.07
[$\bar{1}$ $\bar{1}$ 2]	20.8 + 0.7	0.06	19.5 ± 0.7	0.08

[a] The 95% confidence intervals are all less than ± 0.01.

Comparing the two single crystals, higher plastic deformation initiation loads generally exist for TiO_2 than for SnO_2. This is a contradictory result because TiO_2 is softer than SnO_2 and in terms of deformation might be expected to yield, or to initiate plastic flow at lower indentation test loads. The fact that the resulting W values for the ceramic single crystals reported here are similar to those for the much softer metals reported by Hays and Kendall must also be viewed with some reservation.

The essence of the Hays/Kendall approach is that the ISE is simply an artefact of the indentation test if

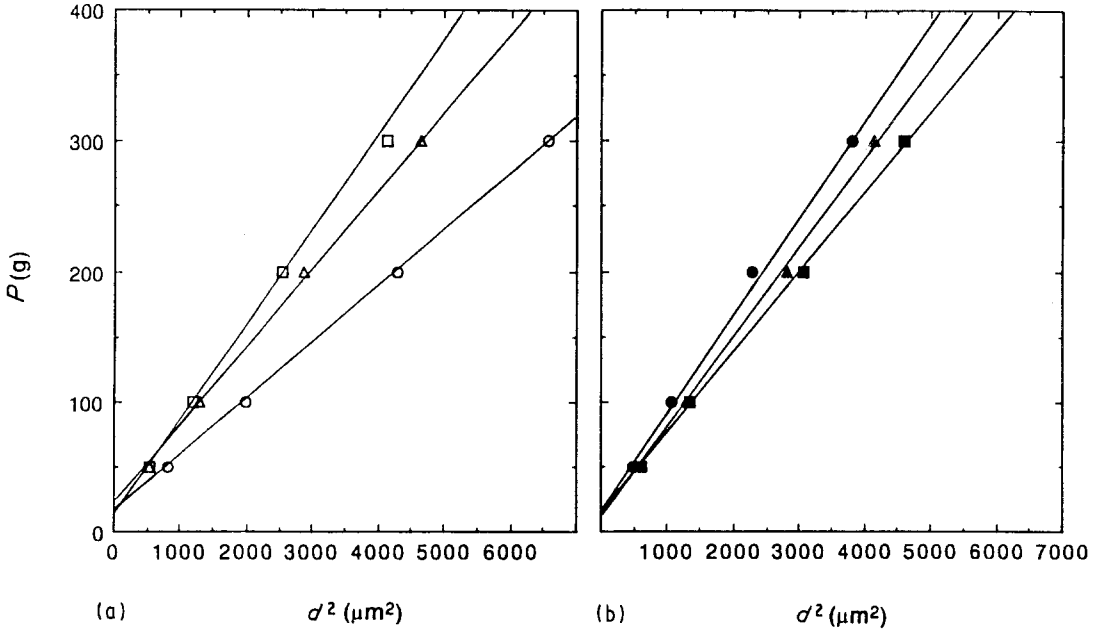

Figure 2 Hays/Kendall approach for the determination of the load for initiation of plastic flow on the (1 0 0) for single crystals of (a) TiO_2 and (b) SnO_2. [0 0 1] W = (□) 16.3 ± 0.7, (■) 18.2 ± 0.6; [0 1 1] W = (△) 21.0 ± 0.8(g), (▲) 10.0 ± 0.7(g); [0 1 0] W = (○) 17.7 ± 0.7, (●) 14.8 ± 0.4.

the effective indentation test load ($P - W$) is considered in the microhardness calculations. The power-law exponent will always be 2 as originally suggested by Kick [1]. Because the W values have now been determined, this point can be examined further through an iteration of Equation 2a in the logarithmic form by treating the exponent as a variable n_w, which yields

$$\log(P - W) = \log(K) + n_w \log(d) \quad (3)$$

The subscript w is applied to the exponent to relate it to the assumption for the calculation of W values. If the indentation load/size effect is from the sample resistance, W, to initiate plastic deformation, the regression analysis of Equation 3 using the previously determined W values should yield n_w values equal to 2 for the experimental microhardness results. Logarithmic plots are presented in Fig. 3 for the (1 0 0) planes of the two crystals. The n_w values of the straight lines appear to be about 2. They are also significantly different from the power-law exponents of Equation 1 summarized in Table I. As Hays and Kendall previously concluded, it is also tempting to conclude that the material-resistance load to initiate plastic flow may be the cause of the ISE. However, close scrutiny of the results suggests otherwise.

Table III summarizes all the n_w values as determined through the iteration of Equation 3 along with the 95% confidence intervals based on the "t" distribution for these crystals. There exists significant deviation between the experimental n_w values and 2 when the Hays/Kendall approach is applied. In fact, all of the n_w values are larger than 2. This suggests that the ISE cannot be explained simply by taking the deformation initiation resistance, W, into account, as has been suggested by Hays and Kendall. In addition, if an original n value of less than 2 indicates that the apparent microhardness increases with a decrease of indentation test load, then n_w values greater than two indicate the opposite. This is obviously not the experimental result that has been observed for the single crystals of TiO_2 and SnO_2 [10, 11].

TABLE III Exponents n_w for the Hays/Kendall approach in single crystals of TiO_2 and SnO_2

$(h\ k\ l)[u\ v\ w]$	TiO_2	SnO_2
(1 0 0)		
[0 0 1]	2.08 ± 0.08	2.10 ± 0.06
[0 1 1]	2.11 ± 0.07	2.04 ± 0.05
[0 1 0]	2.09 ± 0.08	2.06 ± 0.06
(1 1 0)		
[0 0 1]	2.12 ± 0.07	2.06 ± 0.06
[1 $\bar{1}$ 1]	2.18 ± 0.06	2.09 ± 0.05
[1 $\bar{1}$ 0]	2.22 ± 0.06	2.10 ± 0.06
(0 0 1)		
[1 0 0]	2.24 ± 0.08	2.03 ± 0.05
[1 1 0]	2.07 ± 0.07	2.03 ± 0.07
[0 1 0]	2.20 ± 0.07	2.03 ± 0.06
(1 1 1)		
[1 $\bar{1}$ 0]	2.09 ± 0.07	2.09 ± 0.07
[$\bar{1}$ $\bar{1}$ 2]	2.11 ± 0.07	2.11 ± 0.06

It must be concluded that the Hays/Kendall approach to explain the ISE produces several inconsistencies. First, the calculated W values are much too large with respect to both the experimental indentation test loads and the loads at which the initiation of plastic deformation actually occurs. Significant plastic deformation occurs during indentation at only 50 g, whereas the W values are about 20 g. Test loads creating significant plastic deformation are much less than the W values predicted by the Hays/Kendall analysis. Second, the hardnesses of TiO_2 are lower than those of SnO_2, but the calculated W values for TiO_2 are generally higher than those for SnO_2. A similar problem was also revealed in a study by Kotru *et al.* [9] on aluminates and orthochromites. Finally, although the n_w values are about 2, the summary in Table III clearly establishes that the iteration

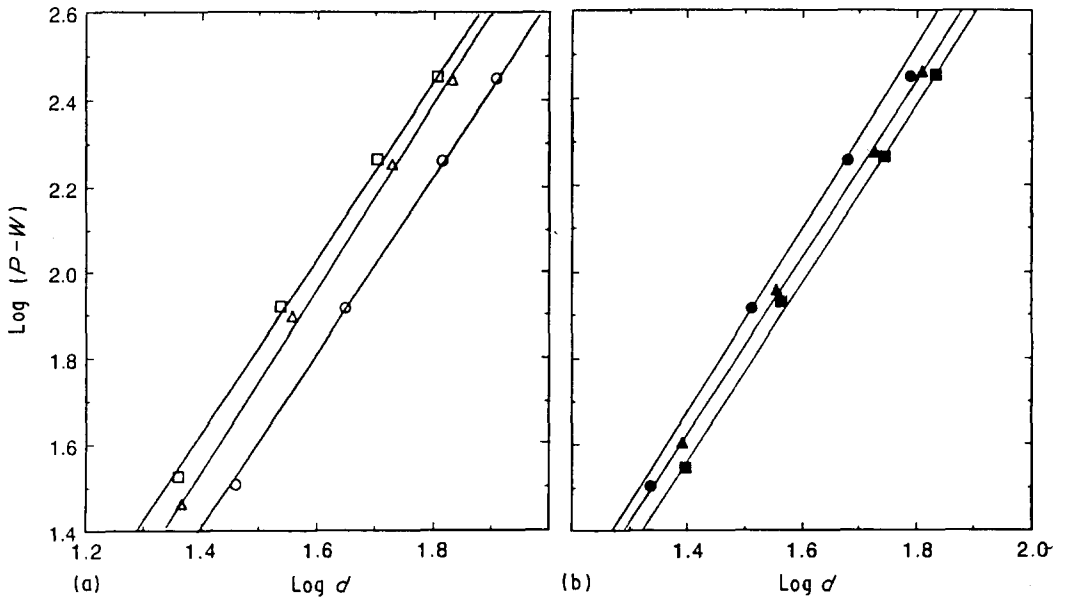

Figure 3 Power-law relationship on the (1 0 0) of the Hays/Kendall approach for single crystals of (a) TiO_2, and (b) SnO_2. [0 0 1] n_w = (□) 2.08 ± 0.08, (■) 2.10 ± 0.06; [0 1 1] n_w = (△) 2.11 ± 0.07, (▲) 2.04 ± 0.05; [0 1 0] n_w = (○) 2.09 ± 0.08, (●) 2.06 ± 0.06.

process does not yield an exponent equal to 2, but one that is consistently greater than 2. It must be concluded that while the Hays/Kendall proposal of the incorporation of the material resistance load for the initiation of plastic flow or yielding may provide for some additional insight to the ISE on the microhardness, it does not provide a satisfactory explanation of the ISE.

2.2. A proportional specimen resistance (PSR) model

An alternative proposal for analysis of the ISE is that the test-specimen resistance is not a constant as proposed by Hays and Kendall, but increases with the indentation size and is directly proportional to it. This is a logical approach for the resistance of the test specimen, P_r, appears to be a directly proportional, elastic-like one as evinced by the unloading curves of instrumented hardness investigations. Load–indentor penetration curves have been recorded for MgO [19], silicon [20], aluminium and steel [20–22]. The unloading regions presented in those studies reveal that the specimen resistance is linearly proportional to the indentor penetration depth and thus the indentation size. Those results justify the assumption that the specimen resistance is directly proportional to the indentation size. The proportional specimen resistance (PSR) can be expressed in the form

$$P_r = a_1 d \tag{4}$$

To a first approximation, the form of Equation 4 can be considered to be similar to the elastic resistance of a spring with the opposite sign to the applied indentation test load. The elastic properties of solids confirm that there must be a linear elastic component to a_1. The indentation size, d, can be related to the indentation depth through the geometry of the indentor.

To evaluate the proposal that the microhardness ISE on the microhardness results from the specimen resistance as expressed by Equation 4, the effective indentation test load is expressed as $(P - P_r)$. The effective indentation load and the indentation size are then related as

$$P - P_r = a_2 d^2 \tag{5}$$

Substituting Equation 4 into Equation 5 yields

$$P = a_1 d + a_2 d^2 \tag{6a}$$

where the a_1 ($g\,\mu m^{-1}$) coefficient relates to the proportional resistance of the test specimen and a_2 ($g\,\mu m^{-2}$) is a constant with units of stress.

Equation 6a is of the same general form that has been applied by Bernhardt [23] and by Frohlich *et al.* [24] when utilizing (reducing) a polynomial series representation of the applied load to the indentation size effect. None of these researchers, however, have attributed the $a_1 d$ term to an indentation-size proportional resistance of the test specimen. Rather they treat the $a_1 d$ term as derived from an $a_1 d^2$ term when divided by d in an energy-balance approach and therefore relate it to a specimen surface energy. Attributing the a_1 term to the specimen surface energy yields unacceptably large surface-energy values, exceeding 10^6 erg cm^{-2}(0.1 J cm^{-2}), as has been discussed by Hirao and Tomozawa for fused silica [25]. Thus, even though Equation 6a has been demonstrated to describe satisfactorily several sets of experimental microhardness results, researchers have been puzzled by the excessive magnitude of the a_1 values. Relating a_1 to the proportional specimen resistance (PSR), rather than a surface energy, provides a new interpretation and also a clear alternative to the unreasonably high surface-energy values.

The proportional specimen resistance (PSR) model described by the a_1 value and the second coefficient, a_2, can be readily evaluated through the linear regression of P/d versus d. Equation 6a in the alternative form is

$$\left(\frac{P}{d}\right) = a_1 + a_2 d \tag{6b}$$

Fig. 4 illustrates P/d versus d for the (1 0 0) planes of the TiO_2 and SnO_2 single crystals. Correlations for these plots are very high, $r^2 > 0.99$. Table IV summarizes all of the a_1 and a_2 values for the two single crystals. Similar to the previous parameters which are descriptive of the microhardness, these a_1 and a_2 values are also anisotropic. It is significant that on the (0 0 1) planes where two equivalent directions have been measured, the [1 0 0] and the [0 1 0], the a_1 and a_2 values for each of the individual crystals are nearly identical.

Having determined the a_1 values and the a_2 values from the experimental results, it is necessary to attribute some physical significance to each, otherwise the PSR model does not provide for any improvement beyond the power-law description. If it is true that the power-law exponent, n, less than 2 is the result of not taking the proportional specimen resistance of the test specimen into account, then it naturally follows that there must exist a correlation between the n values and the a_1 values that describe the proportional specimen resistance (PSR). Fig. 5 depicts the power-law n values versus the proportional specimen resistance a_1 values for the single crystals. It is evident that there exists a strong correlation ($r^2 = 0.94$) between the two quantities which are inversely related. As an n value of 2 should correspond to an a_1 value of 0, it is also significant that the results extrapolate to an n value intercept of 1.97 ± 0.04 for an a_1 value equal to 0. It must be concluded that the a_1 values and the n values are related with respect to the ISE. On an empirical basis, the power-law exponents reflect the observed ISE as a result of curve fitting. However, with respect to the actual indentation process, the physical mechanism which determines the n value is the proportional specimen resistance (PSR) of the test sample which is described by the a_1 value.

The relationship depicted in Fig. 5 confirms that the ISE is a result of PSR. During microhardness indentation the facets of the diamond indentor are aligned with different crystallographic planes and orientations. If the specimen resistance has an elastic component, then it must vary from one crystal plane to another, as well as for different indentor orientations

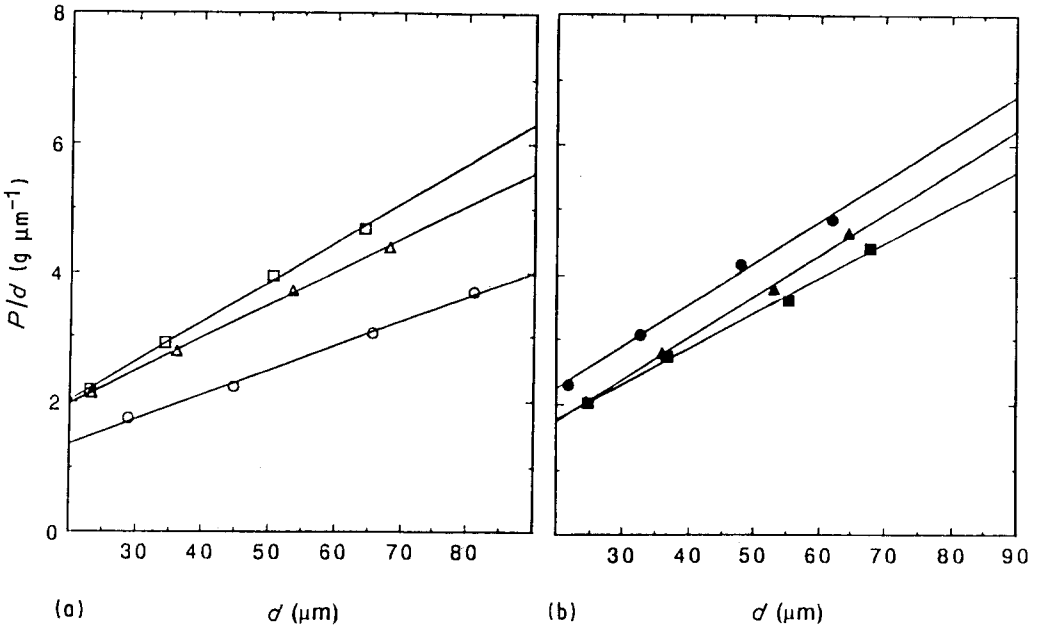

Figure 4 The proportional specimen resistance (PSR) model applied to the (1 0 0) for single crystals of (a) TiO_2, and (b) SnO_2. (□, ■) [0 0 1], (△, ▲) [0 1 1], (○, ●) [0 1 0].

TABLE IV Parameters a_1, a_2 of the PSR model for single crystals of TiO_2 and SnO_2

$(h\ k\ l)[u\ v\ w]$	TiO_2		SnO_2	
	a_1 (g μm^{-1})	a_2 (g μm^{-2})	a_1 (g μm^{-1})	a_2 (g μm^{-2})
(1 0 0)				
[0 0 1]	0.80 ± 0.05	0.061 ± 0.005	0.95 ± 0.03	0.065 ± 0.006
[0 1 1]	0.96 ± 0.02	0.051 ± 0.006	0.44 ± 0.06	0.065 ± 0.005
[0 1 0]	0.62 ± 0.03	0.038 ± 0.006	0.66 ± 0.06	0.055 ± 0.003
(1 1 0)				
[0 0 1]	1.14 ± 0.06	0.061 ± 0.005	0.59 ± 0.01	0.059 ± 0.003
[1 $\bar{1}$ 1]	1.31 ± 0.05	0.049 ± 0.004	0.83 ± 0.02	0.059 ± 0.003
[1 $\bar{1}$ 0]	1.19 ± 0.05	0.047 ± 0.005	0.91 ± 0.02	0.058 ± 0.006
(0 0 1)				
[1 0 0]	1.42 ± 0.04	0.035 ± 0.004	0.30 ± 0.03	0.070 ± 0.004
[1 1 0]	0.67 ± 0.06	0.056 ± 0.004	0.41 ± 0.03	0.083 ± 0.004
[0 1 0]	1.37 ± 0.02	0.036 ± 0.006	0.31 ± 0.05	0.070 ± 0.004
(1 1 1)				
[1 $\bar{1}$ 0]	0.83 ± 0.05	0.052 ± 0.006	0.86 ± 0.04	0.062 ± 0.005
[$\bar{1}$ $\bar{1}$ 2]	0.99 ± 0.05	0.054 ± 0.006	1.01 ± 0.06	0.068 ± 0.003

on the same crystal plane, because the elastic properties are fourth-order tensors and are anisotropic. This appears to be the situation, for when two crystallographic indentation conditions are the same for a specimen, then the a_1 values should be identical with respect to those equivalent conditions. This is confirmed, as the $n_{[100]}$ values are the same as the $n_{[0\ 1\ 0]}$ values on the (0 0 1) planes, as are the $a_{1[1\ 0\ 0]}$ and the $a_{1[0\ 1\ 0]}$ values on the (0 0 1) for these two rutile-structure single crystals.

It is of interest to compare the a_1 values with the elastic moduli of the crystals. The single-crystal elastic constants of rutile and cassiterite have been measured [26, 27], thus the Young's moduli, $E_{\langle h\ k\ l\rangle}$, are readily calculated. Perpendicular to the (1 0 0) planes, the Young's moduli are 147.3 and 174.5 GPa for TiO_2 and SnO_2, respectively, while for the (1 1 0), the values are 368.8 and 368.3 GPa. The (0 0 1) are 385.8 and 340.1 GPa and the (1 1 1) are 318.9 and 278.8 GPa. If the a_1 values are directly proportional to the Young's moduli perpendicular to the planes, then the (1 0 0) planes should have the smallest a_1 values, only about one-half of those of the other three crystal planes. The a_1 values in Table IV do not consistently ascribe to the above order of the Young's moduli. Thus, while the elastic properties of the crystals undoubtedly contribute to the a_1 values and the ISE, the elastic compression of the crystals by the indentor must not be the only contribution to the ISE and the a_1 value.

Having concluded that the $a_1 d$ term is an indentation-size elastic- like proportional resistance of the test specimen, it is of interest to attempt to estimate it

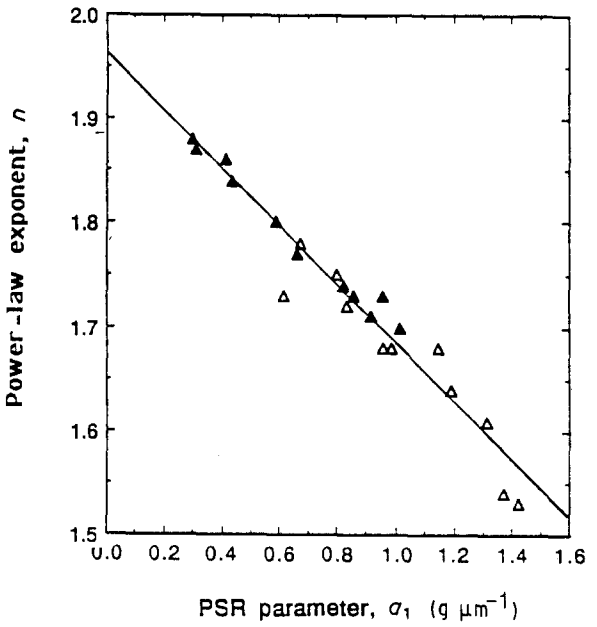

Figure 5 Relationship between the power-law exponent n, and the PSR parameter, a_1, for single crystals of (△) TiO_2 and (▲) SnO_2.

independently. Instrumented microhardness tests that display linear unloading curves have been reported by Doerner and Nix [21], Loubet *et al.* [19] and Pharr and Cook [22]. Order of magnitude estimates of the a_1 term can be made from the initial linear regions of the unloading curves in those publications, although they are for a Berkovich and not a Knoop indentor. The a_1 values estimated from those studies are slightly larger than the experimental a_1 values in Table IV. This discrepancy may occur either from an overestimate of the applied test load, or an underestimate of the indentor penetration depth. As the latter is unlikely, the overestimate must be because of the load discrepancy. It must be concluded that the effective indentation test load is less than the applied test load.

The use of the externally applied test load to estimate a_1 from instrumented indentation unloading curves overestimates its value. This is because the use of the applied load does not consider either the elastic resistance of the test specimen or the diamond facet/specimen interface frictional effects. When a pyramidal indentor is impressed into the test specimen surface, the local contact stresses are very high at the indentor facet/specimen interface. Thus the frictional effects over the area of the contact must also be substantial as suggested by the experiments of Atkinson and Shi [28]. When the frictional force parallel to the indentor facet/specimen interface is resolved into its components, a portion directly opposes the applied test load. Thus the resulting effective indentation load is reduced by the opposing indentor facet/specimen interfacial friction as well as the elastic resistance of the test specimen. This presents the same dilemma that is encountered in attempts to calculate the actual resolved shear stresses on the slip planes beneath and surrounding the indentor when explaining microhardness anisotropy [29]. It is evident that the externally applied test load is reduced by the indentor facet/specimen friction resistance. Its effect should increase as the indentation size decreases because the indentation conditions involve a higher indentation surface to deformation volume. Therefore, the a_1 value consists of two component effects: (i) the elastic resistance of the test specimen, and (ii) the indentor facet/specimen interface friction.

Buckley and Miyoshi [30] have studied the friction of ceramic single crystals. According to their experimental results, the coefficient of friction is a function of both the crystal plane and crystallographic orientation. The coefficient of friction also increases substantially with increasing contact load as Enomoto and Yamanaka report [31]. Those experimental results not only support a significant frictional component of the proportional specimen resistance (PSR) and an anisotropic description of the a_1 values observed in this study, but also its direct proportionality to the applied test load. In retrospect, this should not be surprising as Doerner and Nix [21] have discussed the incorporation of non-linear elasticity to correlate better their instrumented indentation load–depth slopes with the test specimen's elastic properties. They estimated a local hydrostatic stress of nearly 10 GPa beneath the indentor, applying the elastic modulus increase at high pressures to account for the observed experimental discrepancy. The overestimate of the elastic modulus can be similarly explained by the reduction of the applied test load by frictional effects at the indentor facet/specimen interface.

It must be concluded that the a_1 value represents the proportional specimen resistance (PSR) of the test sample. It is possible to demonstrate the relationship of the a_1 value to the original power-law exponent and the ISE. However, it is a formidable challenge to calculate the a_1 value from first principles. This is because the PSR is composed of two components: (i) the elastic resistance of the test specimen, and (ii) the frictional resistance developed at the indentor facet/specimen interfaces. Both contributions may be expected to be anisotropic, but the latter cannot be calculated without the knowledge of the crystallographic and the stress dependencies of the coefficient of friction between the indentor facets and the test specimen.

No relationship exists between the a_2 values and the power-law exponents for these crystals, therefore it is appropriate to reject any direct association of the a_2 values with the ISE. According to Equation 6a and the results of Fig. 5, when $a_1 = 0$ and there is no indentation size effect, the a_2 value must be related to the load-independent hardness. In their investigation of the hardness anisotropy of cubic single-crystal LaB_6, Li and Bradt [32] applied a self-consistent approach to the power law of Equation 1 to obtain

$$P = \frac{2P_c}{n}\left(\frac{d}{d_o}\right)^n \tag{7}$$

where P and d have the same meaning as for the simple power law, and the n value is identical for Equations 1 and 7. d_o is the characteristic indentation size which is derived from the experimental data and P_c is the critical indentation load level, above which the indentation size effect is significantly reduced, or

diminished. Both d_o and P_c are readily obtained from experimental results if data are taken over a sufficiently wide range of microhardness indentation test loads. The d_o and P_c values may be applied through the standard hardness equation when the load-independent hardness, H_o, is determined [32]. Table V lists the d_o and P_c and H_o values for these single crystals. Fig. 6 shows that the load-independent hardness, H_o, is directly related to the a_2 value of the expression for the d-dependence of P in Equation 6. This suggests that there must also exist a correlation between the a_2 value and the quantity P_c/d_o^2. Table VI summarizes and compares the P_c/d_o^2 and a_2 values for TiO_2 and SnO_2. The two are virtually identical. It must be concluded that the a_2 value is physically defined by P_c/d_o^2 and that it is representative of the load-independent hardness, H_o.

Fig. 7a illustrates the microhardness results on the (1 0 0) in the [0 0 1] for both TiO_2 and SnO_2, while Fig. 7b presents a general schematic diagram of the ISE. It is evident that the ISE only contributes to the measured microhardness at test loads less than P_c and indentation sizes below d_o. The ISE increases the measured microhardness above the load-independent hardness value. When the increment of apparent microhardness increase by the ISE is examined for similar test conditions for the two single crystals, for example at the 50 g, (1 0 0) [0 0 1] test condition, then if the indentor facet/specimen interface frictional effects are not too different, the ISE contribution to the hardness increase for the two crystals may be expected to be related to their elastic moduli of the (1 0 0). For SnO_2 and TiO_2, the $E_{(100)}$ are 174.5 and 147.3 GPa, respectively, a ratio of 1.18. The ISE "hardening"

TABLE V The normalized power-law parameters for single crystals of TiO_2 and SnO_2

$(h\ k\ l)[u\ v\ w]$	TiO_2			SnO_2		
	p_c(g)	d_o(μm)	H_o(g mm^{-2})	P_c(g)	d_o(μm)	H_o(g mm^{-2})
(1 0 0)						
[0 0 1]	354 ± 18	75.4 ± 2.6	887 ± 35	379 ± 19	75.5 ± 2.2	946 ± 38
[0 1 1]	303 ± 15	75.7 ± 2.7	751 ± 38	327 ± 16	70.9 ± 2.1	927 ± 46
[0 1 0]	309 ± 16	89.5 ± 3.6	549 ± 22	308 ± 15	74.3 ± 2.2	795 ± 32
(1 1 0)						
[0 0 1]	330 ± 17	72.3 ± 2.2	899 ± 27	375 ± 19	79.0 ± 2.4	855 ± 34
[1 $\bar{1}$ 1]	307 ± 15	77.0 ± 2.4	737 ± 29	314 ± 16	72.0 ± 2.1	864 ± 26
[1 $\bar{1}$ 0]	313 ± 16	79.8 ± 2.3	701 ± 28	292 ± 16	69.3 ± 2.1	867 ± 30
(0 0 1)						
[1 0 0]	289 ± 15	86.3 ± 3.0	553 ± 28	299 ± 15	65.1 ± 2.5	1003 ± 30
[1 1 0]	319 ± 16	75.2 ± 3.1	803 ± 32	320 ± 16	61.7 ± 2.4	1196 ± 36
[0 1 0]	294 ± 14	85.7 ± 3.5	568 ± 20	315 ± 16	66.9 ± 2.3	1002 ± 25
(1 1 1)						
[1 $\bar{1}$ 0]	311 ± 16	76.5 ± 2.4	756 ± 30	305 ± 15	70.4 ± 2.3	898 ± 31
[$\bar{1}$ $\bar{1}$ 2]	290 ± 15	71.9 ± 2.6	798 ± 24	300 ± 15	65.3 ± 2.7	1001 ± 38

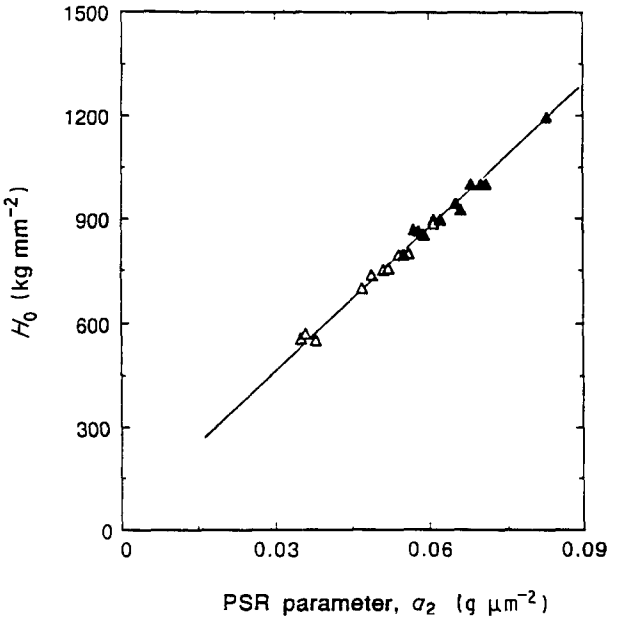

Figure 6 Relationship between the load-independent hardness, H_o, and the PSR parameter, a_2, for single crystals of (△) TiO_2 and (▲) SnO_2.

TABLE VI Comparison of the P_c/d_o^2 and a_2-values for single crystals of TiO_2 and SnO_2

$(h\ k\ l)[u\ v\ w]$	TiO_2		SnO_2	
	(P_c/d_o^2) (g μm^{-2})	a_2-value (g μm^{-2})	(P_c/d_o^2) (g μm^{-2})	a_2-value (g μm^{-2})
(1 0 0)				
[0 0 1]	0.062	0.061	0.065	0.065
[0 1 1]	0.053	0.051	0.065	0.065
[0 1 0]	0.039	0.038	0.056	0.055
(1 1 0)				
[0 0 1]	0.063	0.061	0.060	0.059
[1 $\bar{1}$ 1]	0.052	0.049	0.061	0.059
[1 $\bar{1}$ 0]	0.049	0.047	0.061	0.058
(0 0 1)				
[1 0 0]	0.039	0.035	0.071	0.070
[1 1 0]	0.056	0.056	0.084	0.083
[0 1 0]	0.040	0.036	0.061	0.070
(1 1 1)				
[1 $\bar{1}$ 0]	0.053	0.052	0.062	0.062
[$\bar{1}$ $\bar{1}$ 2]	0.056	0.054	0.070	0.068

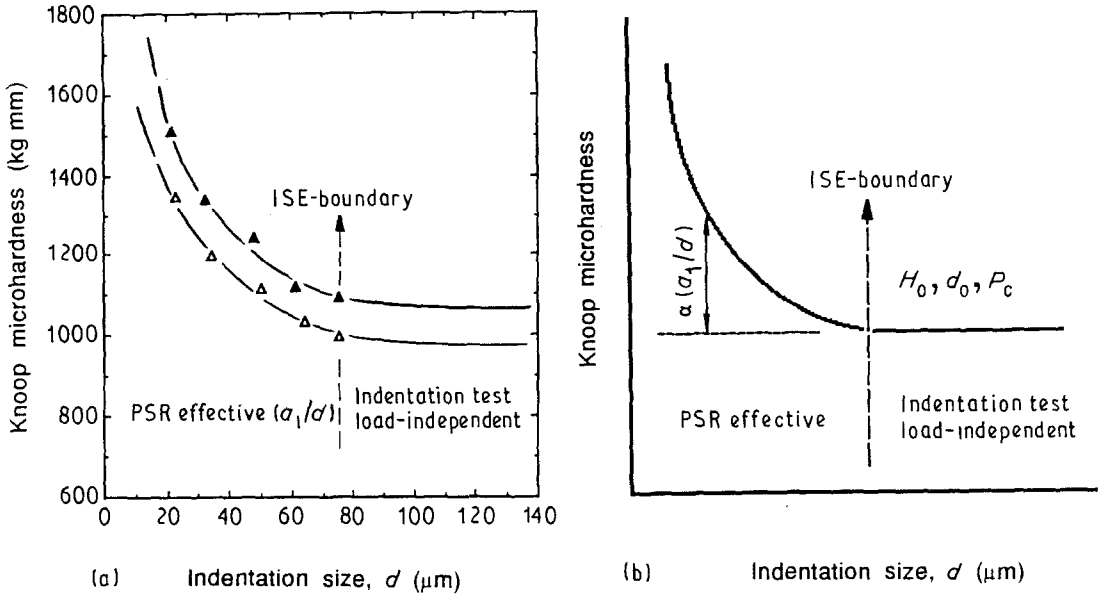

Figure 7 Indentation load/size effect for single crystals of (a) TiO_2 and SnO_2 for the (1 0 0) [0 0 1] crystallographic reference, and (b) a schematic representation of the ISE.

increments at the 50 g test loads are 570 and 460 kg mm^{-2}, respectively, a ratio of 1.23. These ratios are essentially the same, especially considering that the indentor facet/specimen frictional effects are unknown and may be slightly different. This confirms the importance of the specimen elastic modulus contribution to the ISE and the a_1 term.

It is now possible to further specify the a_2 term in Equation 6a. As the a_2 term is just P_c/d_o^2, Equation 6a becomes

$$P = a_1 d + \left(\frac{P_c}{d_o^2}\right) d^2 \tag{8}$$

where the $a_1 d$ term has been previously defined as the proportional specimen resistance (PSR). To express the ISE in terms of the Knoop hardness versus indentation size, Equation 12 can be combined with the standard Knoop microhardness formula

$$\text{KHN} = 14229\frac{P}{d^2} \tag{9}$$

where P is in grams and d is in micrometres, to yield the Knoop microhardness as

$$\text{KHN} = 14229\left[\left(\frac{a_1}{d}\right) + \left(\frac{P_c}{d_o^2}\right)\right] \tag{10}$$

Equation 10 reveals that the Knoop microhardness is composed to two contributions. The first is associated with the ISE as the PSR. It decreases with increasing indentation test load, P, or increasing indentation size, d. The second term is the load-independent hardness contribution, P_c/d_o^2. It depends on the specimen's crystallographic reference and the material, but not on the indentation test load.

According to Equation 10 and consistent with numerous microhardness studies of metals, ceramics and glasses, some in the form of single crystals and some polycrystalline specimens, there exists an indentation load/size effect boundary (ISE-B) which may be specified by P_c and d_o. On the low-test-load side of that boundary, the effect of the PSR on the microhardness is significant and an ISE is prevalent. However, on the high-test-load side, the PSR is insignificant and hence can be neglected in practice.

With respect to the Hays and Kendall concept for the initiation load of plastic flow, W, there would be a term, in Equation 8, similar to the a_0 term of the series originally proposed by Bernhardt [23] and Frohlich *et al.* [24]. However, once W is exceeded, and that appears to occur very early in the indentation process, perhaps at nN test loads, then its contribution is lost in the scatter of the results. The W term may be of practical significance for very low-load-contact friction and wear effects as well as in nanoindentation studies at very low test loads, but it appears to be rather insignificant for normal microhardness measurements.

3. Conclusion

Utilizing experimental data of the Knoop microhardness versus the indentation test load for single crystals of rutile and cassiterite on the (1 0 0), (1 1 0), (0 0 1) and (1 1 1) planes, the indentation microhardness load/size effect (ISE) has been analysed. The power law approach was initially applied, revealing that the indentation load/size effect is anisotropic and varies in extent for single crystals of rutile and cassiterite. In general, single-crystal rutile experiences a greater ISE than single-crystal cassiterite.

A proportional specimen resistance (PSR) model was proposed and applied to explain the ISE. This approach is supported by published experimental results of instrumented micro-/nanohardness studies of the indentation penetration depth versus indentation test load. The PSR model yields the expression

$$P = a_1 d + a_2 d^2 = a_1 d + \left(\frac{P_c}{d_o^2}\right) d^2$$

The a_1 term is related to the power-law exponent, the

n value. It describes the ISE. It was confirmed that the ISE is the result of the proportional specimen resistance (PSR) which is composed of (i) the elastic resistance of the test specimen, and (ii) the friction at the indentor facet/specimen interface.

In the second-order equation describing the test load–indentation size relationship, the a_2 term is not related to the ISE. Rather the a_2 value is descriptive of the load-independent hardness, sometimes referred to as the "true" hardness. It was confirmed that the a_2 term is equal to the quantity P_c/d_o^2 which is defined by the concept of the normalized power-law description of the load–indentation size relationship.

Acknowledgements

The authors thank T. Akiba and H. Ohira, Chichibu Cement Co. Ltd, Kumagaya, Japan, for their assistance with the supply of the rutile single crystals, and S. Marcus, USGS, Reno Office, USA, for his assistance with the supply of cassiterite single crystals.

References

1. F. KICK, Leipzig Felix Edition (1885).
2. H. O'NEILL, "The Hardness of Metals and its Measurement" (Sherwood, Cleveland, OH, 1934) p. 43.
3. B. W. MOTT, "Micro-indentation Hardness Testing" (Butterworths Scientific, London, 1956) p. 101.
4. D. J. CLINTON and R. MORRELL, *Mater. Chem. Phys.* **17** (1973) 461.
5. C. HAYS and E. G. KENDALL, *Metall.* **6** (1973) 275.
6. E. MEYER, *Phys. Z.* **9** (1908) 66.
7. P. M. SARGENT and T. F. PAGE, *Proc. Brit. Ceram. Soc.* **26** (1978) 209.
8. J. T. CZERNUSZKA and T. F. PAGE, *J. Mater. Sci.* **22** (1987) 3907.
9. P. N. KOTRU, A. K. RAZDAN and B. M. WANKLYN, *ibid.* **24** (1989) 793.
10. H. LI and R. C. BRADT, *J. Amer. Ceram. Soc.* **73** (1990) 1360.
11. *Idem, ibid.* **74** (1991) 1053.
12. D. R. TATE, *Trans. ASM* **35** (1945) 374.
13. N. GANE and J. M. COX, *Phil. Mag.* **22** (1970) 881.
14. S. A. VARCHENYA, F. O. MUKTEPAVEL and G. P. UPIT, *Sov. Phys. Solid State* **11** (1970) 2300.
15. G. P. UPIT and S. A. VARCHENYA, in "The Science of Hardness Testing and its Research Applications", edited by J. H. Westbrook and H. Conrad (ASM, Metals, Park, OH, 1973) p. 135.
16. S. J. BULL, T. F. PAGE and E. H. YOFFE, *Phil. Mag. Lett.* **59** (1989) 281.
17. P. M. SARGENT, in "Microindentation Techniques in Materials Science and Engineering", edited by P. J. Blau and B. R. Lawn, ASTM STP 889 (American Society for Testing and Materials, Philadelphia, PA, 1984) p. 160.
18. N. GANE and F. P. BOWDEN, *J. Appl. Phys.* **39** (1968) 1432.
19. J. L. LOUBET, J. M. GEORGES, O. MARCHESINI and G. MEILLE, *J. Tribol.* **106** (1984) 43.
20. J. L. LOUBET, J. M. GEORGES and G. MEILLE, in "Microindentation Techniques in Materials Science and Engineering", edited by P. J. Blau and B. R. Lawn, ASTM STP 889 (American Society for Testing and Materials, Philadelphia, PA, 1984) p. 72.
21. M. F. DOERNER and W. D. NIX, *J. Mater. Res.* **1** (1986) 601.
22. G. M. PHARR and R. E. COOK, *ibid.* **5** (1990) 847.
23. E. O. BERNHARDT, *Z. Metallkde* **33** (1941) 135.
24. F. FROHLICH, P. GRAU and W. GRELLMANN, *Phys. Status Solidi* **42** (1977) 79.
25. K. HIRAO and M. TOMOZAWA, *J. Amer. Ceram. Soc.* **70** (1987) 497.
26. J. B. WACHTMAN Jr, W. E. TEFFT and D. G. LAM Jr, *J. Res. Nat. Bur. Stand. A Phys. Chem.* **66A** (1962) 465.
27. E. CHANG and E. K. GRAHAM, *J. Geophys. Res.* **80** (1975) 2595.
28. M. ATKINSON and H. SHI, *Mater. Sci. Tech.* **5** (1989) 613.
29. C. A. BROOKES, J. B. O'NEILL and B. A. W. REDFERN, *Proc. R. Soc. Lond.* **A322** (1971) 73.
30. D. H. BUCKLEY and K. MIYOSHI, *Wear* **100** (1984) 333.
31. Y. ENOMOTO and K. YAMANAKA, in "Ceramics Databook", edited by S. Saito and H. Yanagida (Gordon and Breach, New York, 1987) p. 299.
32. H. LI and R. C. BRADT, *Mater. Sci. Engng* **A142** (1991) 51.

Received 26 June 1991
and accepted 30 June 1992